Reprinted from the Journal of the American Chemical Society, 1994, *116*.

Self-Assembly through Hydrogen Bonding: Preparation and Characterization of Three New Types of Supramolecular Aggregates Based on Parallel Cyclic $CA_3 \cdot M_3$ "Rosettes"

John P. Mathias, Christopher T. Seto, Eric E. Simanek, and George M. Whitesides*

Contribution from the Department of Chemistry, Harvard University, Cambridge, Massachusetts 02138

Received July 8, 1993. Revised Manuscript Received December 6, 1993®

Abstract: Reaction of hub$(MM)_3$, a compound containing six melamines, with monomeric, dimeric, and trimeric derivatives of isocyanuric acid yields three new types of hydrogen-bonded self-assembled supramolecular aggregates. These new aggregates are represented by hub$(MM)_3$:3benz$(CA)_2$ and hub$(MM)_3$:3furan$(CA)_2$, hub$(MM)_3$:6neohex(CA), and hub$(MM)_3$:3neohex(CA):C_{18}hub$(CA)_3$. These supramolecular aggregates comprise 4–7 individual molecules and have molecular weights in the range 4.1–6.3 kDa. Each aggregate is stabilized by 36 hydrogen bonds in two parallel cyclic $CA_3 \cdot M_3$ "rosettes". Characterization of these aggregates by ^1H and ^{13}C NMR spectroscopies, gel permeation chromatography, and vapor pressure osmometry confirms that each exists as a stable, well-defined structure in chloroform or methylene chloride solutions. The design of these self-assembled aggregates, their relative stabilities, and the techniques used for their characterization are discussed. The operation of positive cooperativity in the self-assembly of hub-$(MM)_3$:6neohex(CA) is demonstrated. The self-assembly of hub$(MM)_3$:3neohex(CA):C_{18}hub$(CA)_3$ demonstrates the controlled aggregation of *three* different components into a single supramolecular aggregate. The size and stability of these self-assembled aggregates are correlated with results obtained from gel permeation chromatography.

Introduction

We are preparing a series of self-assembled supramolecular aggregates based on the hydrogen-bonded lattice formed from cyanuric acid and melamine (CA·M).[1-6] Exploring the design, preparation, and characterization of self-assembled aggregates is important in assessing the value of self-assembly as a strategy in synthesis.[7-10] Recent demonstrations of self-assembly have been reported in other systems: prominent examples include helicates,[11,12] catananes,[13] rotaxanes,[14,15] and other hydrogen-bonded structures.[16-18]

We have shown that hydrogen-bonded supramolecular aggregates based on parallel $CA_3 \cdot M_3$ "rosettes"—such as those represented schematically by structure **1** in Figure 1—are stable in chloroform, methylene chloride, and *o*-dichlorobenzene. These aggregates illustrate many of the features in design and analysis that characterize self-assembled systems.[2,5] In this paper we describe the design and synthesis of hub$(MM)_3$ (**12**), a compound containing six covalently linked melamines that are preorganized to recognize six isocyanurates (CA) to form supramolecular aggregates of 36 hydrogen bonds based on the stacked $CA_3 \cdot M_3$ rosette motif. Hub$(MM)_3$ is represented schematically by structure **2** in Figure 1.

We discuss the preparation and characterization of three new types of self-assembled supramolecular aggregates (having molecular weights ranging between 4.1 and 6.3 kDa) formed between hub$(MM)_3$ (**12**) and isocyanurate derivatives that differ in the number and geometry of their isocyanurates. These aggregates have been characterized by ^1H and ^{13}C NMR spectroscopies, COSY, NOESY and 1-dimensional nuclear Overhauser effect (NOE) measurements, gel permeation chromatography (GPC), and vapor pressure osmometry (VPO). Our objectives in this work were (i) to increase our understanding of molecular self-assembly by preparing a new series of large structures stabilized by 36 hydrogen bonds; (ii) to increase the stability of the aggregates by reducing the entropy of translation opposing self-assembly; (iii) to illustrate the operation of positive cooperativity in assemblies based on parallel $CA_3 \cdot M_3$ rosettes; (iv) to increase the level of selectivity demonstrated in these self-assembly processes by incorporating three different components in a single self-assembled aggregate; and (v) to address trends in relative stability and behavior in solution emerging from the aggregates we have prepared.

Results

Design and Synthesis of Hub$(MM)_3$ (12). The synthesis of hub$(MM)_3$ (**12**) is shown in Scheme 1. This molecule is a progression in structure from hub$(M)_3$, the molecule we have

* Abstract published in *Advance ACS Abstracts*, February 1, 1994.

(1) Seto, C. T.; Whitesides, G. M. *J. Am. Chem. Soc.* **1993**, *115*, 905–916.
(2) Seto, C. T.; Mathias, J. P.; Whitesides, G. M. *J. Am. Chem. Soc.* **1993**, *115*, 1321–1329.
(3) Seto, C. T.; Whitesides, G. M. *J. Am. Chem. Soc.* **1993**, *115*, 1330–1340.
(4) Seto, C. T.; Whitesides, G. M. *J. Am. Chem. Soc.* **1990**, *112*, 6409–6410.
(5) Seto, C. T.; Whitesides, G. M. *J. Am. Chem. Soc.* **1991**, *113*, 712–713.
(6) The structure of the hydrogen-bonded CA·M lattice has been illustrated in previous publications, see refs 1–5. This structure is a putative one, however, and has not been determined by X-ray crystallography. The X-ray crystal of CA·M·3HCl has been reported, see: Wang, Y.; Wei, B.; Wang, Q. J. *Crystallogr. Spectrosc. Reson.* **1990**, *20*, 79–82. The crystal structure of a discrete $CA_3 \cdot M_3$ "rosette" has been reported, see: Zerkowski, J. A.; Seto, C. T.; Whitesides, G. M. *J. Am. Chem. Soc.* **1992**, *114*, 9473–9475.
(7) Whitesides, G. M.; Mathias, J. P.; Seto, C. T. *Science (Washington, D.C.)* **1991**, *254*, 1312–1319.
(8) Lehn, J.-M. *Angew. Chem., Int. Ed. Engl.* **1990**, *29*, 1304–1319.
(9) Lindsey, J. S. *New J. Chem.* **1991**, *15*, 153–180.
(10) Philp, D.; Stoddart, J. F. *Synlett* **1991**, 445–458.
(11) Baxter, P.; Lehn, J.-M.; DeCian, A.; Fischer, J. *Angew. Chem., Int. Ed. Engl.* **1993**, *32*, 69–72.
(12) Constable, E. C.; Hannon, M. J.; Tocher, D. A. *Angew. Chem., Int. Ed. Engl.* **1992**, *31*, 230–232. Constable, E. C. *Tetrahedron* **1992**, *48*, 10013–10059.
(13) Stoddart, J. F.; *et al. J. Am. Chem. Soc.* **1992**, *114*, 193–208. Chambron, J.-C.; Mitchell, D. K.; Sauvage, J.-P. *J. Am. Chem. Soc.* **1992**, *114*, 4625–4631. Hunter, C. A. *J. Am. Chem. Soc.* **1992**, *114*, 5303–5311.
(14) Ashton, P. R.; Bissell, R. A.; Spencer, N.; Stoddart, J. F.; Tolley, M. S. *Synlett* **1992**, 914–918. Ashton, P. R.; Bissell, R. A.; Spencer, N.; Stoddart, J. F.; Tolley, M. S. *Synlett* **1992**, 923–926.
(15) Manka, J. S.; Lawrence, D. S. *J. Am. Chem. Soc.* **1990**, *112*, 2440–2442. Harada, A.; Li, J.; Kamada, M. *Nature* **1992**, *356*, 325–327. Wenz, G.; Keller, B. *Angew. Chem., Int. Ed. Engl.* **1992**, *31*, 197–199.
(16) Bonazzi, S.; DeMorais, M. M.; Gottarelli, G.; Mariani, P.; Spada, G. P. *Angew. Chem., Int. Ed. Engl.* **1993**, *32*, 248–250. Bonner-Law, R. P.; Sanders, J. K. M. *Tetrahedron Lett.* **1993**, *34*, 1677–1680.

0002-7863/94/1516-1725$04.50/0

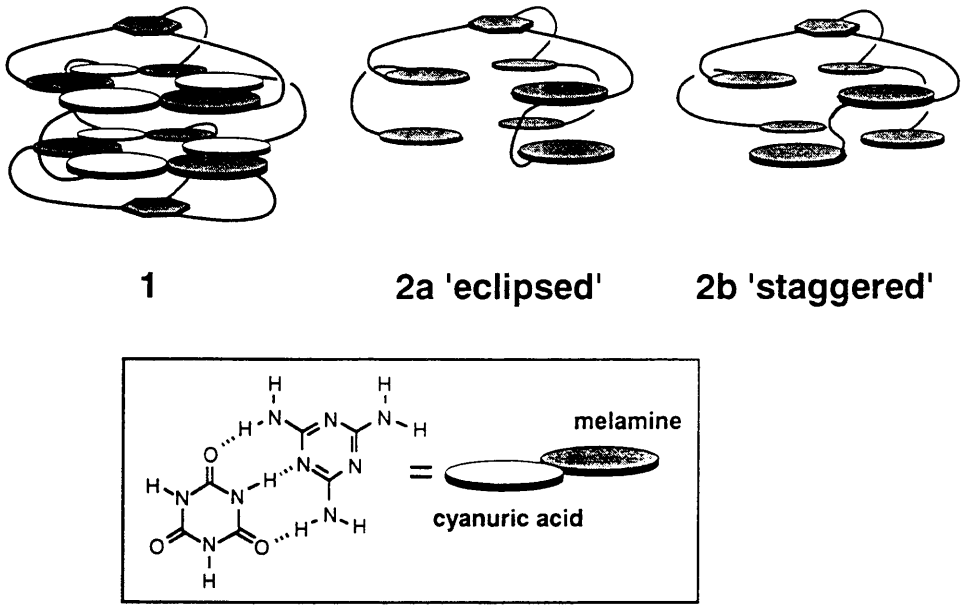

Figure 1. Schematic structures of a previously reported supramolecular aggregate based on two parallel $CA_3{\cdot}M_3$ rosettes (**1**), and hub$(MM)_3$, a compound containing six melamine rings, in eclipsed (**2a**) and staggered (**2b**) conformations.

used as a covalent scaffold in previous self-assembling supramolecular aggregates.[1-5] Hub$(MM)_3$ was designed to afford a stable self-assembled aggregate based on two parallel $CA_3{\cdot}M_3$ rosettes by covalently connecting six melamines into a single molecule. This molecule incorporates three characteristics in structure we have identified to be important in forming the supramolecular aggregates we reported previously.[1-5] First, the linker arm of the "hub" orients the upper melamine in the correct position to allow assembly of the first $CA_3{\cdot}M_3$ rosette. Second, the *m*-xylyl linkage between the two melamines in each arm of **12** provides a spacing between parallel $CA_3{\cdot}M_3$ rosettes we know to be acceptable from previous aggregates. Third, steric hindrance associated with the methyl substituents on the *m*-xylyl linker helps to orient the two melamines in each arm in the direction required for formation of the hydrogen-bonded network.

The synthetic route to **12** is based on a facile preparation of oligomers of melamine. This route takes advantage of the highly selective, stepwise substitution of nucleophiles on cyanuric chloride. Reaction of the first amine occurs at 0 °C; the second occurs at ~5–45 °C, depending on the nature of the amine. Substitution with the third amine (or "NH_2" in the form of NH_4-OH in a sealed tube) can be achieved at 70–120 °C. This procedure prepares unsymmetrically-substituted derivatives of melamine in yields >80% in <24 h. In combination, these procedures make cyanuric chloride a versatile building block in the preparation of the precursors to hydrogen-bonded systems based on polymelamines.

The *m*-xylyl spacer between the two adjacent melamines in each arm of **12** was adapted from benz$(CA)_2$ (**13**), the bisisocyanurate derivative we have used previously to make supramolecular aggregates based on two cyclic $CA_3{\cdot}M_3$ rosettes.[2,5] Linking two melamines this way, however, introduces a level of complexity in the conformation of **12** that is absent in **13**. The unsymmetrical attachment of the xylyl group means that the MelNH–R bonds can rotate to give structures in which the two melamines can be fully eclipsed (**2a**), fully staggered (**2b**), or offset somewhere between these two extremes (Figure 1). The conformation adopted by aggregates formed between **12** and rigid bisisocyanurates (such as **13** and **14**) will be the eclipsed one: this conformation is dictated by the rigid eclipsed conformation of the bisisocyanurate. Aggregates between **12** and monomeric isocyanurates (such as **17**) can, however, adopt multiple different conformations. The correlations between structural features of the precursors and the subsequent structural integrity of supramolecular aggregates derived from them are important aspects in the design of self-assembling systems.

Preparation of Supramolecular Aggregates between Hub$(MM)_3$ (12) and Bisisocyanurate Derivatives—Hub$(MM)_3$:3benz$(CA)_2$ (15) and Hub$(MM)_3$:3furan$(CA)_2$ (16). The supramolecular aggregates hub$(MM)_3$:3benz$(CA)_2$ (**15**) and hub$(MM)_3$:3furan-$(CA)_2$ (**16**) were assembled by reaction between 1 equiv of **12** and 3 equiv of **13** or **14** (Scheme 2A). Both **15** and **16** were prepared by forming a suspension of **12** and the respective bisisocyanurate derivatives in a solution of methanol in chloroform (~1:9 v:v), sonicating the suspension briefly, and heating the suspension at ~40 °C until the mixture became homogeneous (~10 s). Concentration of this mixture to dryness *in vacuo* gave the supramolecular aggregates **15** and **16** as white solids. These fully assembled supramolecular aggregates were soluble in chloroform without the addition of any further methanol. In each case, 1 equiv of **12** solubilized up to, and no more than, 3 equiv of the bisisocyanurate derivative **13** or **14**. This feature provides strong evidence that the relative stoichiometries between the hexamelamine and bisisocyanurate components in **15** and **16** are 1:3.

Characterization of Hub$(MM)_3$:3benz$(CA)_2$ (15) and Hub-$(MM)_3$:3furan$(CA)_2$ (16) by NMR Spectroscopy. The aggregates **15** and **16** were characterized by ^1H and ^{13}C NMR spectroscopies, H→D exchange, COSY, and 1- and 2-D NOE experiments. Spectra of uncomplexed **12** and of the supramolecular aggregates **15** and **16** are shown in Figure 2a–c. Figure 3 assigns specific protons and NOEs in **15**. NOE interactions observed between the imide protons of the isocyanurates and those of the melamine NHs on **12** are strong (they are negative) and consistent with the structures we propose for **15** and **16**. We do not see NOEs between protons in parallel $CA_3{\cdot}M_3$ rosettes. CPK models suggest that the distance between these layers is approximately 4.8 Å.

The spectrum of **12** in $CDCl_3$ (Figure 2a) is broad and featureless. This appearance may be a result of self-association and/or hindered rotation about the amide bonds in this molecule. In contrast, the spectra of **15** (Figure 2b) and **16** (Figure 2c) both show a sharp set of resonances that has been assigned to a *single* supramolecular aggregate. The sharpening of signals on assembly of the aggregate is consistent with the transition from flexible,

(17) Geib, S. J.; Vicent, C.; Fan, E.; Hamilton, A. D. *Angew. Chem., Int. Ed. Engl.* **1993**, *32*, 119–121. Yang, J.; Fan, E.; Geib, S. J.; Hamilton, A. D. *J. Am. Chem. Soc.* **1993**, *115*, 5314–5315.

(18) Zimmerman, S. C.; Duerr, B. F. *J. Org. Chem.* **1992**, *57*, 2215–2217.

Scheme 1. Synthesis of Hub(MM)$_3$ (**12**)[a]

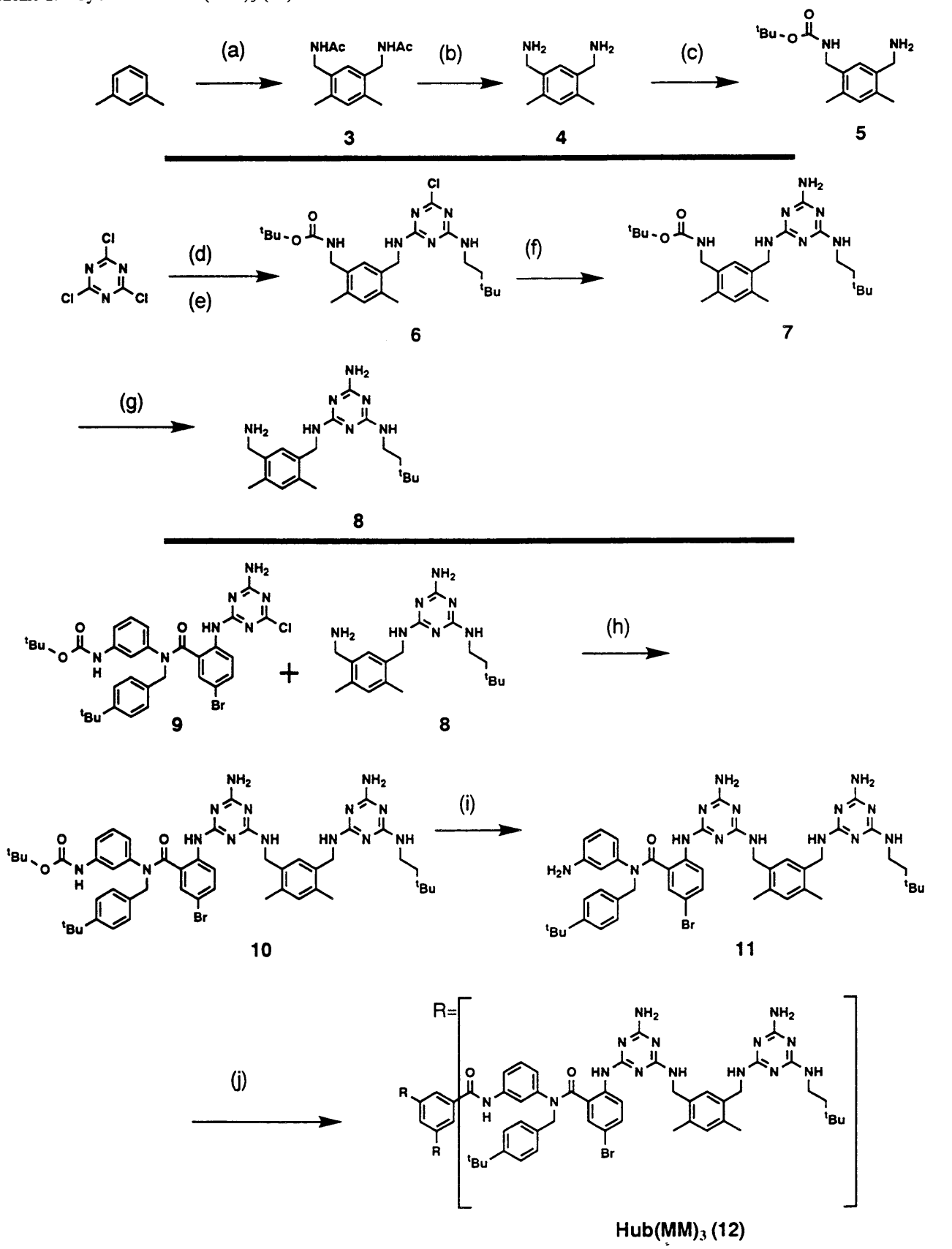

[a] Reagents: (a) paraformaldehyde, MeCN, AcOH, H_2SO_4, 90 °C, 20 h; 29%; (b) 3 N HCl_{aq}, reflux, 20 h; 95%; (c) $(Me)_3COCO_2N{=}C(Ph)CN$ (Boc-ON), DMF, Et_3N, 25 °C, 0.5 h; 51%; (d) neohexylamine, diisopropylethylamine (DIPEA), THF, 0 °C, 10 min; (e) amine **5**, 45 °C, 2 h; (f) 1,4-dioxane, NH_4OH (30% aqueous solution), 120 °C, 7 h, Parr vessel; 88%; (g) TFA, CH_2Cl_2, 25 °C, 2 h; 94%; (h) dimethylacetamide, DIPEA, 90 °C, 4 h; 58%; (i) TFA, CH_2Cl_2, 25 °C, 2 h; 96%; (j) 1,3,5-benzenetricarbonyl chloride, CH_2Cl_2, DIPEA, 25 °C, 0.75 h; 83%.

poorly organized molecule **12** to the highly structured aggregates **15** and **16**. This progression from a broad, featureless spectrum to a sharp set of signals for the complex is also seen in the ^{13}C NMR spectra. Signals for both complexed and uncomplexed components are visible before a full 3 equiv of **13** has been added to **12**.

Scheme 2. Self-assembly of 1 Equiv of Hub(MM)$_3$ (**12**) with (A) 3 Equiv of Benz(CA)$_2$ or Furan(CA)$_2$ To Give Hub(MM)$_3$:3benz(CA)$_2$ (**15**) or Hub(MM)$_3$:3furan(CA)$_2$ (**16**), respectively, (B) 6 Equiv of Neohex(CA) To Give Hub(MM)$_3$:6neohex(CA) (**18**), and (C) 1 Equiv of Hub(CA)$_3$ and 3 Equiv of Neohex(CA) To Give Hub(MM)$_3$:3neohex(CA):C$_{18}$hub(CA) (**20**)

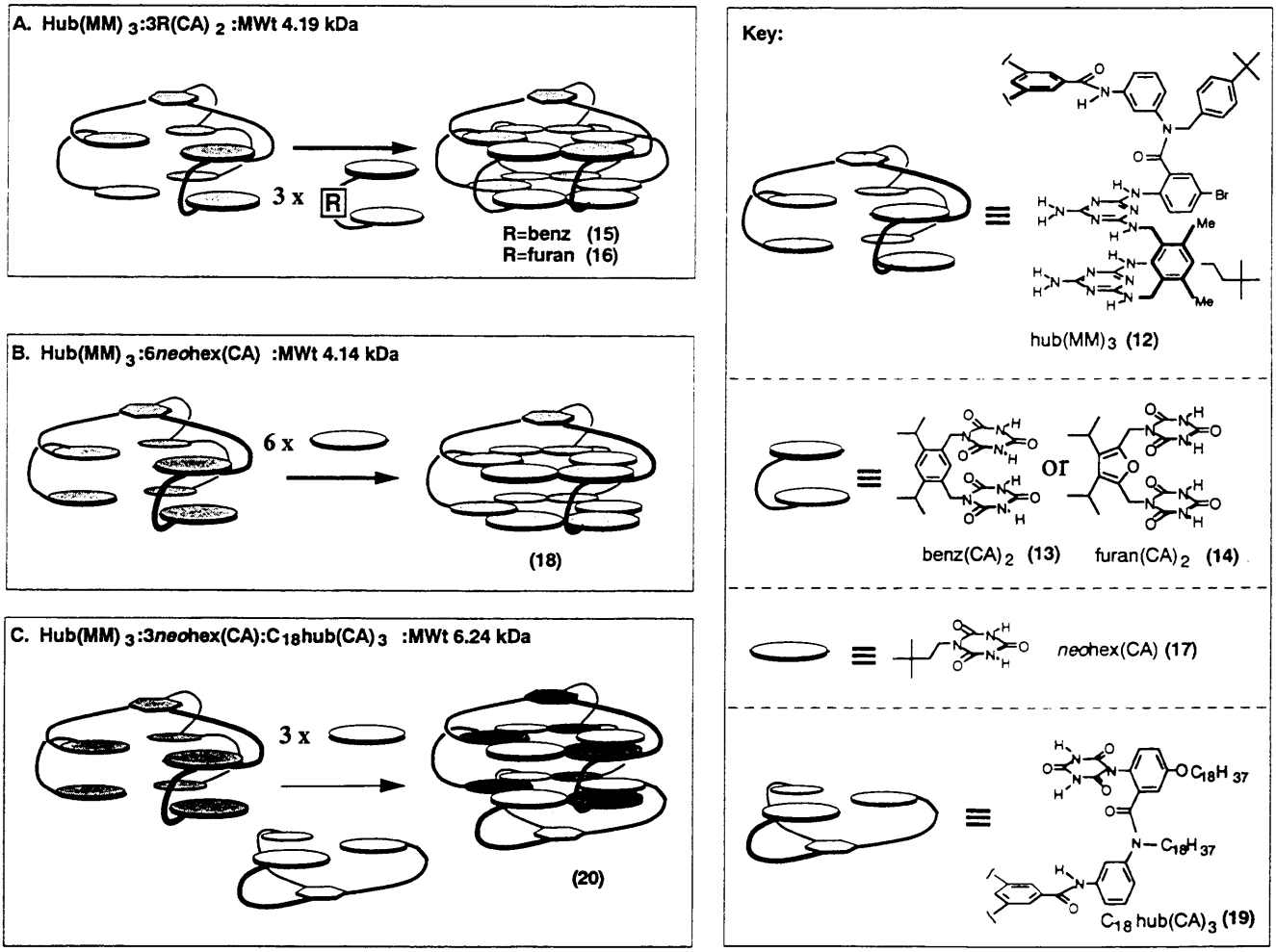

Several features in the NMR spectrum of **15** support the assignment of its structure. First, the observation of four resonances for the isocyanurate protons (H^{1-4}, 14–16 ppm) indicates that two CA_3·M_3 rosettes are included in the structure, with each CA_3·M_3 rosette containing two different types of isocyanurate protons as a consequence of the unsymmetrical substitution of the melamines. In both **15** and **16**, the relative intensities of H^{1-4} are 1:1:1:1, as judged by integration. The line shapes of the resonances for H^{1-4} in **15** are dependent on temperature. This observation suggests that changes in the local structure and dynamics are occurring. The same trend in peak shapes for H^{1-4} is visible in the resonances of the isocyanurate protons in **16**, although the differences are not as large as those in **15**. Second, two strong singlets are observed for the two methyl groups on the *m*-xylyl linker (H^r, H^v, 2.0–2.2 ppm): the linker thus has a well-defined "top" and "bottom" in the aggregate. Third, several sets of protons on **12** become diastereotopic on formation of **15** or **16** (g,g′/q,q′/u,u′/z,z′).

To assess the stabilities of these aggregates in progressively more polar solvents, methanol-d_4 and DMSO-d_6 were titrated into solutions of **15** and **16** in $CDCl_3$. The resonances for the imide protons on the bisisocyanurate derivatives and the NH protons on **12** disappear immediately (<5 min; time to record spectrum) on addition of 5% methanol-d_4 (v:v). This observation indicates that the isocyanurate components of the aggregate are undergoing rapid exchange once significant quantities of methanol are present. The structure of the aggregate, however, is retained in this more polar, hydrogen-bonding medium. Indeed, hub(MM)$_3$:3benz(CA)$_2$ is stable in a solution of methanol-d_4 (up to 20% (v:v)) in $CDCl_3$.[19] Beyond this point, resonances become broad and are no longer consistent with the presence of a well-defined aggregate in solution. The spectrum starts to resemble that of uncomplexed **12**. Changes in the spectra of hydrogen-bonded aggregates on addition of polar solvents provide a qualitative indication of the dynamics and stability of the aggregate. The fact that both **15** and related aggregates of type **1** (Figure 1) based on two parallel CA_3·M_3 rosettes retain their structure in solutions of up to 20% methanol in chloroform suggests that the stabilities of these two types of supramolecular aggregate are qualitatively similar. While it is not possible to predict which of the two aggregates, **15** or 2hub(M)$_3$:3benz(CA)$_2$ (type **1**), might be the more stable by this procedure, both are more stable than previously reported hub(M)$_3$:3(CA) aggregates (which dissociate in 5% MeOH/$CDCl_3$). Samples of **15** in $CDCl_3$ show no change by NMR over a period of 3 weeks. The single set of well-defined peaks associated with **16** are joined by extra resonances that are broad and less well-defined than those of **16**. This difference in stability may be a direct consequence of imperfect complementarity between the *m*-xylyl linkers in **12** and the furanyl linker in **14** and **16**.[20]

(19) This mixture corresponds to a solution of 4.9 M methanol in 9.9 M chloroform. The concentration of the aggregate was 5 mM.

(20) The resonances that appear do not suggest the formation of another discrete aggregate. Instead, the new signals are broad and poorly-defined and account for no more than 20% of the final mixture. We have no evidence to suggest that this behavior is the result of reaction between any of the components in **16** and atmospheric oxygen or trace acidity. No other aggregates display similar time-dependent behavior/instability.

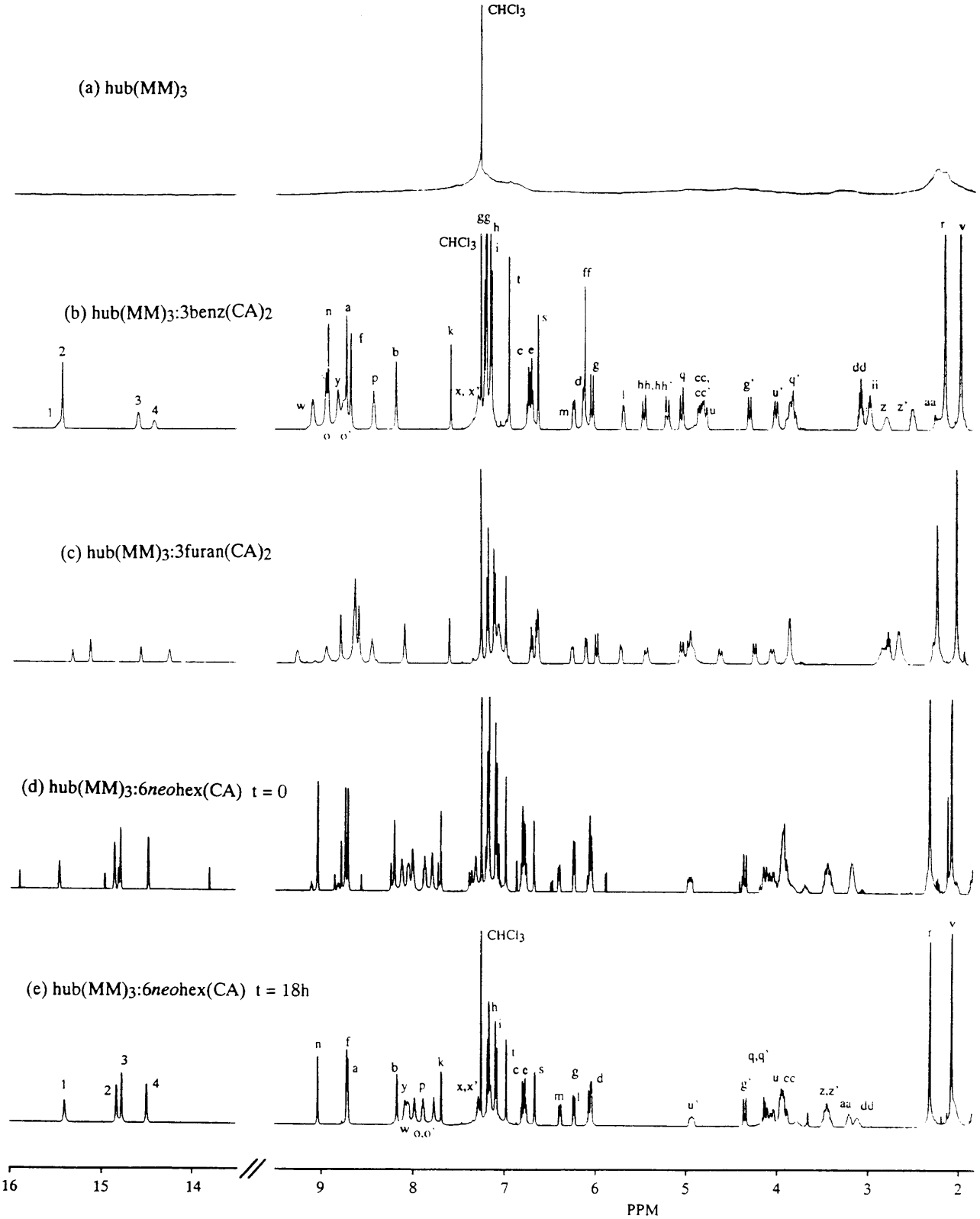

Figure 2. ^{1}H NMR spectra of self-assembled aggregates formed by hub(MM)$_3$ (**12**) (500 MHz, $CDCl_3$).

Characterization of Hub(MM)$_3$:3benz(CA)$_2$ (15) and Hub-(MM)$_3$:3furan(CA)$_2$ (16) by Gel Permeation Chromatography (GPC). Traces from GPC for **15** with CH_2Cl_2 and $CHCl_3$ as the eluent are shown in Figure 4.[21] In each case, *p*-xylene (shaded peak) was used as an internal standard. Retention times of the peaks for **15** with $CHCl_3$ (8.4 min) and CH_2Cl_2 (8.5 min) as the eluent are consistent with the supramolecular structures we propose for **15**. The sharp peak shapes indicate that the relative stabilities of **15** and **16** are also qualitatively similar to those of the aggregates of type **1** (Figure 1).[22]

Characterization of Hub(MM)$_3$:3benz(CA)$_2$ (15) and Hub-(MM)$_3$:3furan(CA)$_2$ (16) by Vapor Pressure Osmometry (VPO). The data obtained for the molecular weights of **15** and **16** in solution by VPO are summarized in Figure 5. In each case, data for the aggregates were calibrated against four independent molecular weight standards. This procedure permits an estimate

(21) The aggregate **16** displays the same behavior in terms of both retention time and peak shape.

(22) Retention times for double layer aggregates of type **1** are 8.4 ($CHCl_3$) and 8.7 min (CH_2Cl_2), see ref 2.

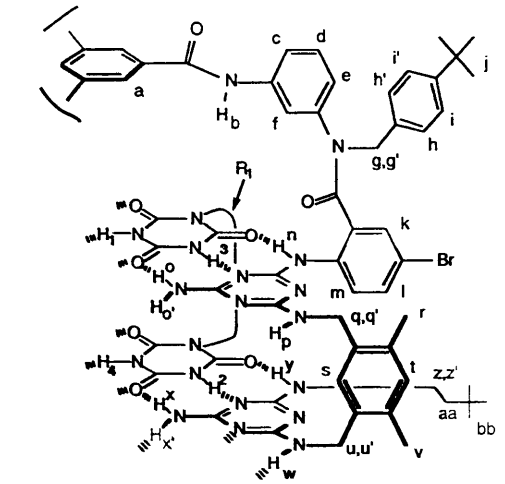

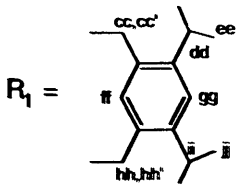

NOE	Intensity
$H_1 \rightarrow H_p$	11%
$H_1 \rightarrow H_{o,o'}$	6%
$H_2 \rightarrow H_y$	18%
$H_2 \rightarrow H_{x,x'}$	11%
$H_3 \rightarrow H_n$	19%
$H_3 \rightarrow H_f$	18%
$H_3 \rightarrow H_{o,o'}$	7%
$H_4 \rightarrow H_w$	18%
$H_4 \rightarrow H_{x,x'}$	16%
$H_{o,o'} \rightarrow H_{1,4}$	8%

Figure 3. Assignment of individual proton resonances and observed NOEs in hub(MM)$_3$:3benz(CA)$_2$ (**15**). Annotations refer to those indicated on Figure 2b. Values reflect direct measurements of the magnitude of NOEs. NOE interactions with intensities below 5% are not listed.

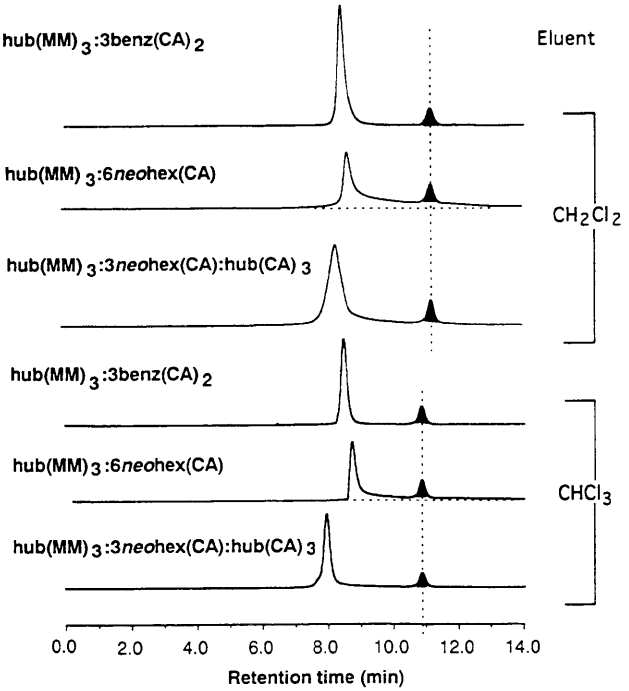

Figure 4. Gel permeation chromatograms of self-assembled aggregates formed by hub(MM)$_3$ (**12**). Shaded peaks are *p*-xylene, which is used as an internal standard. This peak appears at 11.2 min with methylene chloride as the eluent and at 10.9 min with chloroform as the eluent.

of the magnitude of the effects of nonideal behavior of the standards in solution and, therefore, provides a stronger basis with which to interpret data on the aggregates than could be

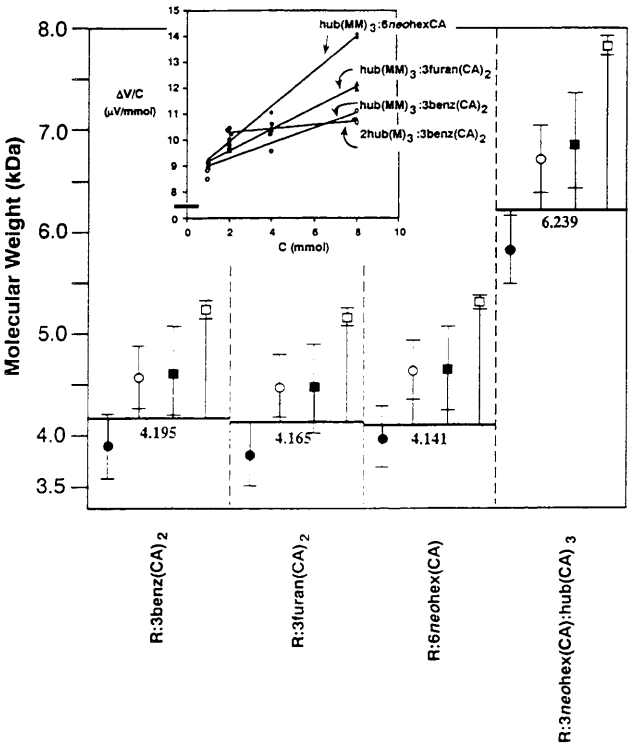

Figure 5. Estimation of the molecular weights in solution by vapor pressure osmometry of four self-assembled aggregates formed by hub(MM)$_3$ (**12**); indicated in the plot by R. Calculated molecular weights for each aggregate are given in each column by solid horizontal bars and associated numbers. In each case, measurements were made against four different standards: *N,N'*-bis-^{t}Boc-gramicidin S (FW 1342) (●), sucrose octaacetate (FW 679) (○), polystyrene (av FW 5050, polydispersity 1.05) (■), and perbenzoyl-β-cyclodextrin (FW 3321) (□). Error bars represent standard deviations of measurements on aggregate and standards. Measurements were made in chloroform at 37 °C with concentrations in the range 1–16 mM. The inset shows the concentration dependence of data from VPO for three self-assembled aggregates based on **12** and one aggregate based on hub(M)$_3$. Lines represent least-squares analyses of these data.

obtained using a single molecular weight standard. The observed molecular weights for **15** and **16** in solution are within 15% of the calculated molecular weights, 4.195 and 4.165 kDa, respectively. This level of agreement is close to that obtained for complexes of type **1** (Figure 1) by VPO.[2,5]

We have examined the concentration dependence of the results obtained from VPO for **15** and **16** (Figure 5, inset). The positive slope of the lines that are obtained is similar to, but more pronounced than, the lines we have obtained for the majority of our complexes. We believe that a negative slope in a plot of ΔV/concentration versus concentration from VPO indicates that concentration-dependent intermolecular association is occurring between the species in solution. We have no consistent rationale, however, to account for the positive slope observed in these cases.[23] We are encouraged by the observation of similar behavior in solution for aggregates (such as **15** and **16**) for which we propose similar global structures.

Preparation of a Supramolecular Aggregate between Hub(MM)$_3$ (12) and a Monomeric Isocyanurate Derivative—Hub-

(23) For a full discussion of the analysis of associating solutes by VPO, including features that influence the slope of traces of (and related to) ΔV/concentration vs concentration, see: Adams, E. T., Jr.; Wan, P. J.; Crawford, E. F. *Methods Enzymol.* **1978**, *48*, 69–154. We note that progressive dissociation of the aggregates **15**, **16**, and **18** into their components as the concentration increased would raise the number of particles in solution above that expected and, therefore, effect a larger change in the vapor pressure than expected. This phenomenon would account for the positive slope in traces of ΔV/concentration vs concentration. This explanation, however, seems unlikely as aggregates less stable than **15** and **16** have exhibited slight negative slope in plots of ΔV/concentration vs concentration.

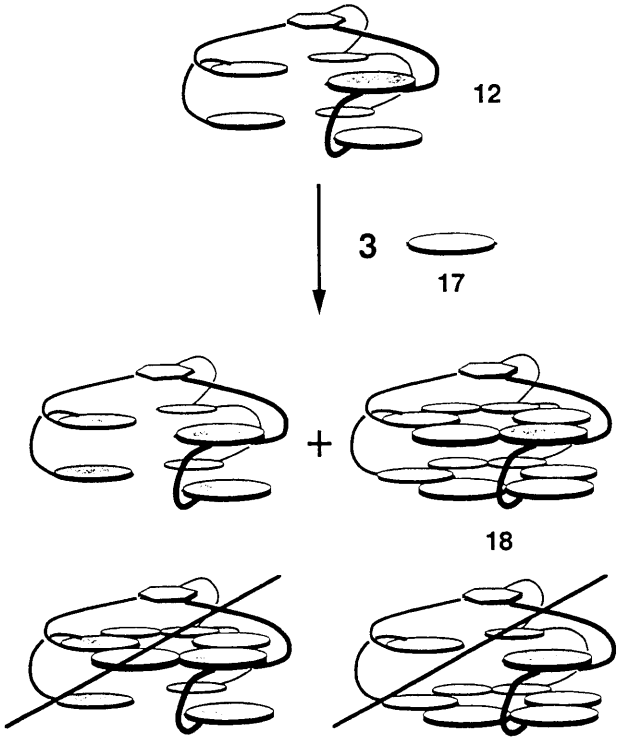

Figure 6. The result of mixing 1 equiv of **12** with 3 equiv of **17**: formation of only **18** along with uncomplexed **12**. We do not see any evidence for the presence of partially-formed aggregates (of the sort shown at bottom), as judged by ^{1}H NMR spectroscopy.

(MM)$_3$:6neohex(CA) (18). A homogeneous solution of hub-(MM)$_3$:6neohex(CA) (**18**) was prepared by mixing **12** and the isocyanurate derivative neohex(CA) (**17**) in chloroform (Scheme 2B). In this case, **12** solubilized up to, and no more than, 6 equiv of **17**. Formation of a single aggregate from the components takes approximately 18 h at room temperature (~1 min at reflux).

Addition of only 3 equiv of **17** to 1 equiv of **12** leads to formation of only the fully-assembled aggregate **18** (Figure 6). Excess **12** remains uncomplexed. Unlike any of the self-assembly processes we have reported previously, the assembly of **18** could generate competing self-assembled aggregates in which only one CA_3·M_3 rosette forms. We would expect these aggregates to have well-defined structures, and we should, therefore, be able to observe these intermediates by ^{1}H NMR if they were present in solution. The fact that we do not observe any of these partially-assembled aggregates *en route* to **18** suggests strongly that the assembly of **18** displays positive cooperativity. The ability to predict and introduce structural features that impart positive cooperativity to a self-assembly process increases greatly the size and complexity of aggregates that can be envisaged using this approach.

Characterization of Hub(MM)$_3$:6neohex(CA) (18) by NMR Spectroscopy. ^{1}H NMR spectra of **18** at t = 0 and after equilibration (t = 18 h at 25 °C) are shown in Figure 2d and e. The progression from a poorly-defined set of signals to a sharp, single set of signals over this interval is consistent with the progression to a structure that is increasingly well-ordered. Expanded portions of the spectra, covering the resonances associated with the hydrogen-bonded isocyanurate protons, are shown in Figure 7b. Initially, two independent sets of four resonances are visible (● and *) for the isocyanurate protons (Figure 7b). We believe that **18** exists initially as a mixture of two conformations in which the relative orientations of the melamines in adjacent layers are both "eclipsed" and "staggered" (see Figure 7a). Resonances of specific protons and NOEs in the final structure of **18** are shown in Figure 8. These data confirm the geometry of the hydrogen-bonded CA_3·M_3 rosettes and are consistent with the structure we propose for **18**. Each CA_3·M_3 rosette gives two resonances for the two different isocyanurate

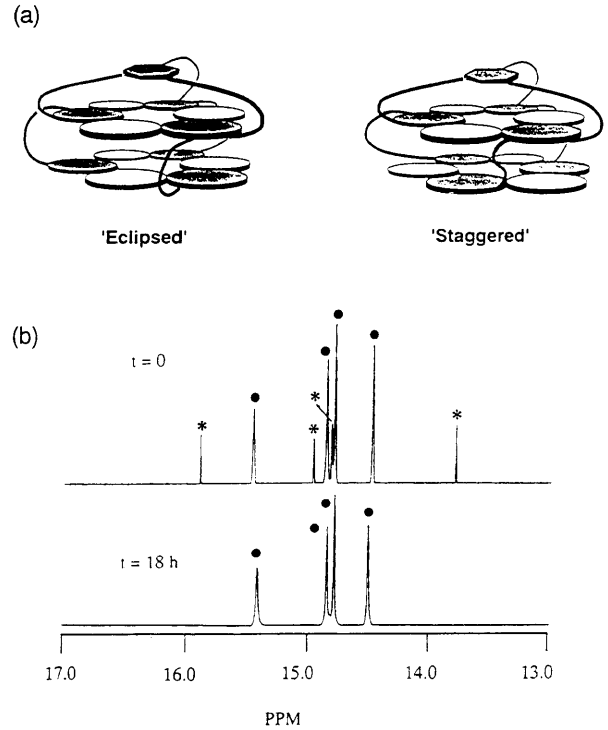

Figure 7. (a) Two possible conformations for hub(MM)$_3$:6neohex(CA) (**18**) that differ in the relationships between the two parallel cyclic CA_3·M_3 rosettes. (b) Expanded portion of the NH isocyanurate region of the ^{1}H NMR spectra of hub(MM)$_3$:6neohex(CA) (**18**) at t = 0 and t = 18 h. The spectrum at t = 0 exhibits two distinct sets of four resonances (● and *) for the four different isocyanurate protons in **18**, suggesting the presence of both eclipsed and staggered conformations. Equilibration over 18 h results in the presence of only one preferred conformation (●).

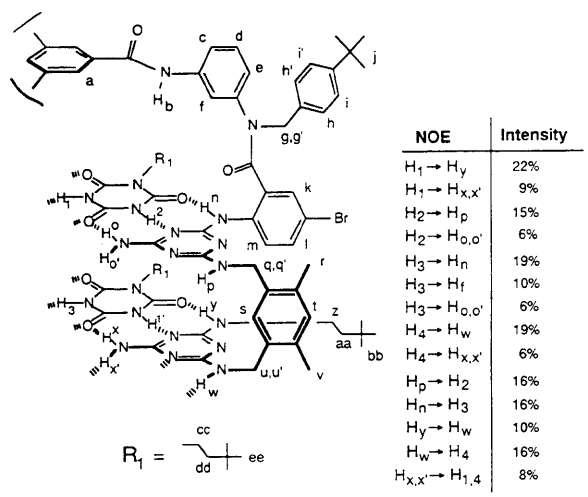

Figure 8. Assignment of individual proton resonances and observed NOEs on hub(MM)$_3$:6neohex(CA) (**18**). Annotations refer to those indicated on Figure 2e. Values reflect direct measurements of the magnitude of NOE interactions. NOE interactions with intensities below 5% are not listed.

protons as a consequence of the unsymmetrical substitution of the melamines. The observation of resonances for both conformations means that exchange between these two states is slow on the NMR time scale. After an interval (~18 h at 25 °C or minutes at 50 °C), only a single conformation of aggregate **18** is present, and the resonances marked with an asterisk disappear. Variable-temperature ^{1}H NMR illustrates that the single set of resonances persists as the temperature is decreased and confirms that the signals at 25 °C are not the product of a time-averaged exchange between different conformers. Unlike **15**, the aggregate **18** does not have a link between the adjacent CA_3·M_3 rosettes that is sufficiently rigid conformationally to dictate the relative

orientation of the $CA_3 \cdot M_3$ rosettes. We would, therefore, expect to see multiple conformations of the aggregate **18**. The observation of a single conformation for **18** after equilibration is surprising. We cannot establish which structure is preferred. The persistence of just one conformation is consistent with the hypothesis that this aggregate based on two parallel $CA_3 \cdot M_3$ rosettes is more stable than those based on a single $CA_3 \cdot M_3$ rosette.

In contrast to **15**, addition of 5% MeOH (v:v) to a solution of **18** in $CDCl_3$ results in the complete loss of structure of the aggregate and dissociation into the separate components, as judged by ^1H NMR. This observation suggests that **18** is less stable than **15**. As both **15** and **18** are stabilized by 36 hydrogen bonds, the lower stability of **18** with seven components is to be expected.

Characterization of Hub(MM)$_3$:6neohex(CA) (18) by GPC. The GPC traces for **18** show a "sharp" peak that displays significant tailing in both $CHCl_3$ (t_R = 8.50 min) and CH_2Cl_2 (t_R = 8.88 min) (Figure 4). The sharp leading edge of these traces is consistent with observations made for **15**. We believe that tailing in GPC is a consequence of dissociation over the duration of the analysis.[24,25] The observation of tailing for **18** further suggests that the stability of this aggregate is lower than that of **15** under the conditions of GPC. The relative stability of **18**, as judged by GPC, is, however, significantly greater than we would have predicted from the trace recorded for hub(M)$_3$:3neohex(CA) (see Figure 10b for structure).

Characterization of Hub(MM)$_3$:6neohex(CA) (18) by VPO. The estimated molecular weight of **18** in solution is within 15% of the calculated molecular weight (Figure 5). The concentration dependence of these data is illustrated in Figure 5, inset. The positive slope of the line in the plot of ΔV/concn versus concn for **18** is similar to those observed for **15** and **16**.

Preparation and Characterization of a Supramolecular Aggregate Composed of Hub(MM)$_3$, Neohex(CA), and a Trivalent Derivative of Isocyanuric Acid, C_{18}hub(CA)$_3$—Hub(MM)$_3$:3neohex(CA):C_{18}hub(CA)$_3$ (20). A supramolecular aggregate was prepared by mixing **12** and two different isocyanurate derivatives in chloroform to afford a suspension. This suspension became a homogeneous solution on being heated gently. Formation of a single aggregate from this mixture took ~48 h at 40 °C. The major initial (kinetic) product of this assembly process is the aggregate **18**. We believe that the final (thermodynamic) product of this process, however, is an aggregate of composition hub(MM)$_3$:3neohex(CA):C_{18}hub(CA)$_3$ (**20**) (Scheme 2C).[26]

The retention times and shapes of the peaks for the aggregate of composition **20** in GPC, with both $CHCl_3$ and CH_2Cl_2 as the eluent, provide evidence that the size of this aggregate is consistent with observations from other self-assembled aggregates in this series. Both traces show a sharp single peak with retention times of 7.9 ($CHCl_3$) and 8.2 (CH_2Cl_2) min (Figure 4). There is a slight degree of broadening associated with the peaks that may be a consequence of the dissociation of the neohex(CA) components. The traces from GPC suggest, however, that the stability of this aggregate lies between that of hub(M)$_3$:3neohex(CA) (top trace) and **20**. The molecular weight we have obtained for **20** in solution is within 20% of the calculated molecular weight (Figure 5).[27]

Discussion

Correlation of Peak Shape in GPC with Relative Stabilities of Self-Assembled Supramolecular Aggregates. Gel permeation chromatography is a useful technique for the analysis of noncovalently bound aggregates in organic solution. Separation occurs primarily on the basis of hydrodynamic radius rather than on the relative strength of absorption on the stationary matrix. The aggregate must, however, have sufficient kinetic stability to remain intact over the 7–9 min required for elution.

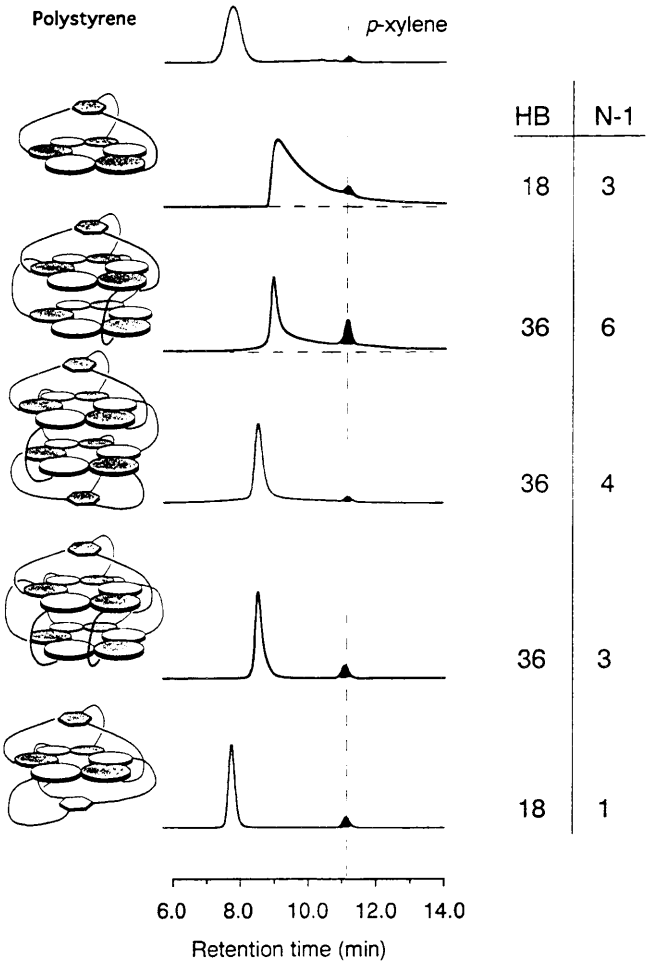

Figure 9. Gel permeation chromatograms of a range of self-assembled aggregates arranged in order of decreasing peak width (and, we believe, stability against dissociation) from top to bottom. Shaded peaks are *p*-xylene, which is used as an internal standard. The eluent in each case was CH_2Cl_2. HB refers to the number of hydrogen bonds stabilizing each aggregate. The parameter ($N-1$) refers to the change in the number of particles on assembly of the aggregate. The top trace is for polystyrene (FW 5050, polydispersity 1.05) and is included to provide a reference.

Figure 9 shows traces from GPC for a range of self-assembled supramolecular aggregates with CH_2Cl_2 as the eluent. In each case, the leading edge (short retention time) of the peak is sharp. This observation suggests that no stable larger hydrogen-bonded assemblies of these aggregates (dimers/trimers) are present in solution. The top trace in Figure 9 is for polystyrene (FW 5050, polydispersity 1.05). Comparison of the retention time in this trace with those in traces for the self-assembled aggregates illustrates the similarity in the sizes of the aggregates. A comparison of the line width of the peak for polystyrene with those of the aggregates suggests that the polydispersities of the stable aggregates are significantly below the 5% quoted for the polystyrene standard. These observations are strong evidence

(24) Johnson, J. F., Ed. *J. Polym. Sci., Part C: Polym. Symp.* **1968**, *21*, 1–344.

(25) Stevens, F. J. *Biochemistry* **1986**, *25*, 981–993. Stevens, F. J. *Biophysics J.* **1989**, *55*, 1155–1167.

(26) Hub(MM)$_3$:3neohex(CA):C_{18}hub(CA)$_3$ can also be prepared by dissolving the three components in a 10% solution of methanol in chloroform and heating (~30 s) to afford a homogeneous solution. Concentration of this solution *in vacuo* gave a white solid that was readily soluble in chloroform. This material is indistinguishable from that obtained by the first procedure.

(27) Mixing equimolar portions of **12** and **19** does not form the well-defined self-, assembled aggregate hub(MM)$_3$:C_{18}hub(CA)$_3$. By making the bottom layer of **12** more rigid with **19**, we hoped to afford an aggregate having a well-defined cavity and, therefore, one that was capable of molecular recognition. ^1H NMR spectroscopy does not, however, provide any evidence for the formation of a structured aggregate between **12** and **19**. In this case, GPC does show the presence of a broad peak with retention time ~7–8 min. The nature and shape of this peak are not consistent with the presence of a well-defined supramolecular aggregate. We are currently examining several other methods of generating self-assembled aggregates possessing cavities.

for the existence of all these self-assembled supramolecular aggregates as well-defined, discrete structures in solution. We can also deduce that nonspecific self-association between discrete aggregates to generate stable larger assemblies is not a major feature of the behavior of these supramolecular structures in solution at concentrations used for analysis in GPC (0.1–1 μM).

The tailing to longer retention time in some of the traces is a consequence of dissociation of the aggregate on the column during analysis.[25] Once a fully-assembled supramolecular aggregate has dissociated during the analysis into a range of smaller structures by progressive loss of isocyanurates, the components would be separated by the column and recombination of the aggregate would be impossible. The extent of tailing in traces from GPC represents, therefore, a qualitative indication of the stability of the self-assembled aggregate under the conditions used for analysis. Comparison of the traces should allow the relative stabilities of aggregates to be determined and form the basis for testing models to predict the stabilities of new aggregates.

The aggregates in Figure 9 are arranged in order so that the ratio of hydrogen bonds stabilizing the aggregate (HB) to the change in the number of particles ($N-1$) increases from top to bottom.[28] A clear trend from board traces with tailing (top) to sharp peaks (bottom) is visible in these traces from GPC. This trend *observed* from GPC correlates qualitatively with that of increasing stability we *predict* for the aggregates by considering the fundamental enthalpic (HB) and entropic ($N-1$) features of the self-assembly process in each case.[29] This progression in increasing stability is consistent with observations made on diluting solutions of the aggregates with hydrogen-bonding solvents.

Retention Times in GPC Correlates with the Molecular Weights of Self-Assembled Supramolecular Aggregates. Figure 10a shows a plot of the observed retention times of self-assembled aggregates in GPC against ln[molecular weight]. In each case the eluent was CH_2Cl_2. A series of polystyrene standards is included (open circles) in this plot for reference. In this figure, ln[molecular weight] and retention time by GPC are correlated. Taking all of the supramolecular aggregates together (with the possible exception of F), longer retention times are observed than would be expected for a polystyrene standard of the same molecular weight. The simplest explanation for this increase in retention time for types A–E is that the aggregates are more compact (that is, they have higher density) than the polystyrene standards.

In greater detail, aggregates containing one M_3·CA_3 sheet (a monorosette) and those containing two (bisrosettes) may have different trend lines with slopes roughly equal to one another but significantly smaller than that for polystyrene. We show these lines on Figure 10a but caution that the slopes and lines may be artifacts of a small set of data. The difference between these lines would be compatible with the interpretation that the bisrosettes were more compact than the monorosettes. In particular, the behavior of the aggregate of type F may be anomalous. This aggregate is formed between 1 equiv of a trismelamine derivative (*h*-flex$(M)_3$) and 1 equiv of a trisisocyanurate derivative (C_{18}hub$(CA)_3$) (Figure 10b). This aggregate is the most lipophilic of those included in the plot. The trisisocyanurate portion of F bears six octadecyl chains, and the trismelamine portion has the highest content of lipophilic groups and is one of the most flexible of the structures we have used. These features may combine to increase the hydrodynamic radius of the aggregate. Correlation between molecular weight and retention time by GPC is not straightforward. The different chemical nature of the outer parts of these aggregates—some having octadecyl chains, some with lipophilic linker arms, some with more polar linker arms, some with their CA_3·M_3 rosettes exposed to solvent, and some with the CA_3·M_3 rosettes hidden from the solution—makes the observation of a modest degree of scattering in the results for these aggregates unsurprising.

Conclusions

The enthalpy associated with the formation of 36 hydrogen bonds in two parallel CA_3·M_3 rosettes, such as hub$(MM)_3$:6neohex(CA) (**18**), is sufficient to overcome the unfavorable entropy of association of seven particles in a single supramolecular aggregate. The stability of the self-assembled aggregates based on hub$(MM)_3$ (**12**) decreases as the ratio of the number of hydrogen bonds stabilizing the aggregate to the number of components increases. This trend can be expanded to include all of the self-assembled aggregates we have reported to date. The ability to correlate the *observed* stability with the *predicted* stability of supramolecular aggregates contributes to understanding the thermodynamics of self-assembly and the features important in the design of supramolecular aggregates.

Data from VPO provide acceptable molecular weights in solution for these aggregates and indicate that hub$(MM)_3$:3benz$(CA)_2$ (**15**), hub$(MM)_3$:3furan$(CA)_2$ (**16**), and hub$(MM)_3$:6neohex(CA) (**18**) are nonideal solutes. Their behavior is, however, mutually consistent (they display the same types of nonidealities). We can conclude that these closely-related supramolecular structures are behaving in a similar fashion in solution.

A slight mismatch between linking units in the bisisocyanurate derivative (**14**) and hub$(MM)_3$ (**12**) affects the thermodynamic stability of the aggregate derived from them (**16**). While hub$(MM)_3$:3benz$(CA)_2$ (**15**) appears to exhibit no decomplexation over time, hub$(MM)_3$:3furan$(CA)_2$ (**16**) dissociates significantly, albeit slowly, with time.

The formation of a single conformation for the aggregate of composition hub$(MM)_3$:6neohex(CA) (**18**) suggests that there are strong preferences for one particular conformation (eclipsed or staggered) over the other possible conformation. This feature is important in allowing characterization of this aggregate. The self-assembly of hub$(MM)_3$:6neohex(CA) (**18**) displays positive cooperativity. This observation suggests that it will be possible to construct supramolecular aggregates that are stabilized by more than two parallel CA_3·M_3 rosettes.[30] Furthermore, the sharpness of the peak for hub$(MM)_3$:6neohex(CA) (**18**) in GPC demonstrates that this aggregate is more stable than would have been expected from the trace of hub$(M)_3$:3neohex(CA).

Assembly of a supramolecular aggregate of composition hub$(MM)_3$:3neohex(CA):C_{18}hub$(CA)_3$ (**20**) demonstrates that *three different* types of components can be incorporated into a single self-assembled aggregate. The ability to perform self-assembly between *many* different types of molecules, selectively and reliably, rather than just two different types of molecules, will ultimately allow the preparation of supramolecular structures that are significantly larger and more complex than those reported in this paper.

Experimental Section

General Methods. NMR experiments were performed with a Bruker AM 500 instrument. Elemental analyses were performed by Spang Microanalytical Laboratory. THF was distilled from sodium benzophenone ketyl. Methylene chloride and triethylamine were distilled from calcium hydride. Dimethylformamide was dried and stored over 4-Å

(28) This ratio can be throught of as a simple, approximate empirical parameter that relates stability to the favorable enthalpy of formation associated with the self-assembly of the aggregate (related to HB) and to the magnitude of the unfavorable reduction in entropy of translation associated with the assembly process (related to $N-1$). As the ratio of HB/($N-1$) increases, intuition predicts an increase in the stability of the supramolecular aggregate. The parameter HB/($N-1$) is not a form that can be justified thermodynamically, but it is useful for comparing structures qualitatively.

(29) We are developing a more rigorous model to predict and relate enthalpic and entropic contributions to self-assembly processes: Mammen, M.; Whitesides, G. M. Unpublished results.

(30) We have recently observed the self-assembly of 10 particles into a single supramolecular aggregate based on three parallel CA_3·M_3 rosettes, see: Mathias, J. P.; Simanek, E. E.; Seto, C. T.; Whitesides, G. M. *Angew. Chem., Int. Ed. Engl.* Submitted.

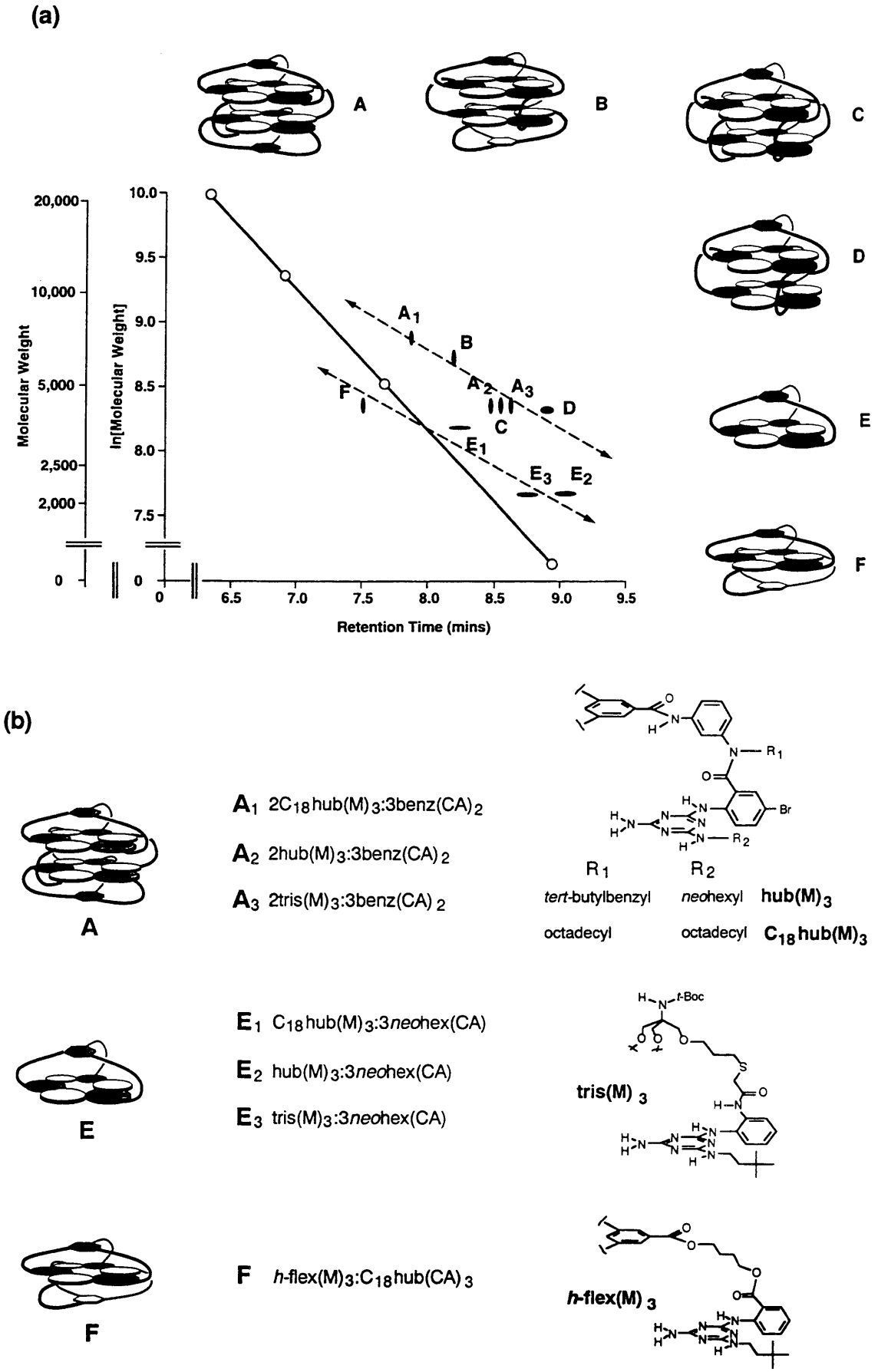

Figure 10. (a) Plot showing the correlation between ln[molecular weight] and retention time in GPC for a range of self-assembled aggregates. Open circles are for polystyrene standards. Vertical solid dots indicate that the aggregate shows no tailing in GPC. Horizontal solid dots indicate that the aggregate shows tailing in GPC. CH_2Cl_2 was the eluent in all cases. (b) The molecular structures of the aggregates included in Figure 10a. In each case the isocyanurate molecules were neohex(CA) (**17**), benz$(CA)_2$ (**15**), and C_{18}hub$(CA)_3$ (**19**). The structures of these molecules are given in Scheme 2.

molecular sieves. The compounds that have a triazine unit in their chemical structures show doubling of several resonances in their ^1H and ^{13}C NMR spectra due to slow exchange of conformers around the NHR–triazine bonds.

NOE Spectra. The NOE spectra of these supramolecular aggregates were recorded at 25 °C, with an evolution period of 3.0 s and a relaxation delay of 6.0 s. The complex (5.0 μmol) was dissolved in 0.7 mL of $CDCl_3$, and the sample was degassed with five freeze–pump–thaw cycles.

Gel Permeation Chromatography. Gel permeation chromatography was performed using a Waters 600E HPLC with a Waters 484 UV detector and a Waters analytical gel permeation column (Ultrastyragel, 1000-Å pore size). Elutions were performed at room temperature using HPLC grade CH_2Cl_2 or $CHCl_3$ (containing *p*-xylene (3.0 mM) as an internal reference) as the eluent at a flow rate of 1.0 mL/min. The samples were prepared at concentrations of 0.125 mM for the complexes and 0.25 mM for free hub(MM)$_3$. The injection volume was 20 μL.

Molecular Weight Determinations by Vapor Pressure Osmometry. Molecular weight determinations were made with a Wescan Model 233 vapor pressure osmometer operated at 35 °C. The molecular weights of the complexes were measured in HPLC grade glass distilled chloroform at concentrations of approximately 1, 2, 4, 8, and 16 mM. At each concentration, 3–4 measurements were taken. Calibration curves were generated using four molecular weight standards: sucrose octaacetate (MW 679), perbenzoyl-β-cyclodextrin (MW 3321), polystyrene (MW 5050, polydispersity 1.05), and a derivative of gramicidin S in which the two ornithine amino groups had been converted to their *tert*-butylcarbamates (MW 1342).

Specific Procedures. *N,N'*-Diacetyl-1,3-bis(aminomethyl)-4,6-dimethylbenzene (3). This compound was synthesized according to the procedure of Parris and Christenson.[31] A 1-L 3-necked round-bottomed flask equipped with a pressure-equalizing addition funnel and a reflux condenser was charged with 200 mL of glacial acetic acid, 45 mL of concentrated sulfuric acid, and 25.0 g (800 mmol) of powdered 95% paraformaldehyde. The mixture was heated at 50 °C in an oil bath for 15 min until all the solid was dissolved. The mixture was cooled to 30 °C, and acetonitrile (42 mL, 800 mmol) was added dropwise to the mixture, keeping the temperature between 60–65 °C. After the spontaneous reaction was completed, *m*-xylene (200 mmol) was added to the mixture, and the reaction was heated at 90 °C for 20 h. The reaction mixture was cooled to room temperature, diluted with water (100 mL), and concentrated *in vacuo* to ~120 mL. The residue was diluted with water (200 mL) and cooled in an ice bath. This solution was stirred vigorously and made basic (pH ~ 12) with 10 N NaOH. The precipitate was collected by vacuum filtration, washed with 1 L of water, and dried in an oven (~110 °C) for 24 h. The product was recrystallized from MeOH (two crops), giving 28.4 g (114.5 mmol, 29%) of the title compound as a white solid after drying under high vacuum: ^1H NMR (400 MHz, DMSO-d_6) δ 8.09 (t, J = 5.2 Hz, 2 H), 6.97 (s, 1 H), 6.90 (s, 1 H), 4.07 (d, J = 5.3 Hz, 4 H), 2.12 (s, 6 H), 1.78 (s, 6 H); ^{13}C NMR (100 MHz, DMSO-d_6) δ 172.56, 137.89, 135.41, 131.72, 43.82, 26.17, 21.81; HRMS-FAB (M + Na)$^+$ calcd for $C_{14}H_{20}N_2O_2Na$ 271.1422, found 271.1437.

1,3-Bis(aminomethyl)-4,6-dimethylbenzene (4). *N,N'*-Diacetyl-1,3-bis(aminomethyl)-4,6-dimethylbenzene (3) (15 g, 60.2 mmol) was suspended in a 3 N HCl_{aq} (300 mL), and the mixture was heated under an atmosphere of nitrogen at reflux for 20 h. The reaction was cooled in an ice bath, and the solution was made basic (pH ~ 12) with 10 N NaOH. The solution was extracted with CH_2Cl_2 (5 × 200 mL). The organic layer was dried over $MgSO_4$, filtered, and concentrated *in vacuo*. The crude product was taken on to the next reaction without further purification. The crude yield of 4 was 9.4 g (57.3 mmol, 95%): ^1H NMR (400 MHz, DMSO-d_6) δ 7.24 (s, 1 H), 6.85 (s, 1 H), 3.62 (s, 4 H), 2.18 (s, 4 H), 1.72 (br s, 4 H); ^{13}C NMR (100 MHz, DMSO-d_6) δ 142.53, 136.33, 135.03, 130.90, 46.93, 21.62; HRMS-FAB (M + H)$^+$ calcd for $C_{10}H_{17}N_2$ 165.1392, found 165.1395.

***N'*-((*tert*-Butyloxy)carbonyl)-1,3-bis(aminomethyl)-4,6-dimethylbenzene (5).** A solution of diamine 4 (2.5 g, 15.2 mmol) and Et_3N (5 mL) in DMF (75 mL) was stirred at 25 °C. Boc-ON (3.9 g, 15 mmol) was added portionwise over 15 min, during which time the solution turned yellow. After a further 10 min, the solution was concentrated *in vacuo*, and the yellow residue was partitioned between EtOAc (150 mL) and 1 N NaOH (70 mL). The organic extract was washed with 1 N NaOH (75 mL) and brine (2 × 75 mL), dried over $MgSO_4$, filtered, and concentrated *in vacuo*. The residue was purified by column chromatography [eluted with a solution of 5% NH_4OH/MeOH in $CHCl_3$ (1:9 v:v)] to give 2.05 g (7.7 mmol, 51%) of the product as a white solid: ^1H NMR (400 MHz, DMSO-d_6) δ 7.19 (t, J = 5.6 Hz, 1 H), 7.13 (s, 1 H), 6.87 (s, 1 H), 4.04 (d, J = 5.4 Hz, 2 H), 3.62 (s, 2 H), 2.19 (s, 3 H), 2.17 (s, 3 H), 2.10 (br s, 2 H), 1.38 (s, 9 H); ^{13}C NMR (100 MHz, DMSO-d_6) δ 159.32, 142.13, 138.38, 137.12, 136.68, 135.16, 130.48, 81.29, 46.76, 45.00, 31.96, 21.70, 21.63; HRMS-FAB (M + H)$^+$ calcd for $C_{15}H_{25}N_5O_2$ 265.1916, found 265.1910.

2-Chloro-4-(neohexylamino)-6-[(3-((*N'*-((*tert*-butyloxy)carbonyl)amino)methyl)-4,6-dimethylbenzyl)amino]-1,3,5-triazine (6). Neohexylamine (0.38 mL, 2.84 mmol) was added to a solution of cyanuric chloride (552 mg, 3 mmol) and DIPEA (0.7 mL) in THF (25 mL) at 0 °C. After 10 min, TLC showed complete conversion to the mono addition product. The solution was warmed to 45 °C, and the amine 5 (750 mg, 2.84 mmol) was added. The suspension was heated at 45 °C for 2 h, during which time it became homogeneous. The reaction mixture was cooled and concentrated *in vacuo*, and the residue was partitioned between EtOAc (125 mL) and brine (75 mL). The organic extract was washed with brine (70 mL), dried over $MgSO_4$, filtered, and concentrated *in vacuo* to give of the product as a white solid. This product was used without further purification: m/z (positive ion FABMS) 477 for (M + H)$^+$.

2-Amino-4-(neohexylamino)-6-[(3-((*N'*-((*tert*-butyloxy)carbonyl)amino)methyl)-4,6-dimethylbenzyl)amino]-1,3,5-triazine (7). The triazine derivative 6 (1.4 g, 3 mmol) was suspended in 1,4-dioxane (10 mL), and NH_4OH (10 mL) was added. The mixture was sealed in a Parr vessel, and the reaction was stirred at 120 °C for 7 h. After cooling and depressurization, the reaction mixture was concentrated *in vacuo*, and the residue was partitioned between EtOAc (150 mL) and brine (100 mL). The organic extract was washed with brine (50 mL), dried over $MgSO_4$, filtered, and concentrated *in vacuo*. The mixture was purified by column chromatography (eluted with EtOAc) to give 1.19 g (2.65 mmol, 88%) of the product as a white solid: ^1H NMR (400 MHz, DMSO-d_6 δ 7.15 (br m, 1 H), 7.08 (s, 1 H), 6.87 (s, 1 H), 6.76–5.85 (6 × br s, 4 H), 4.37 (br s, 2 H), 4.02 (m, 2 H), 3.14 (br m, 2 H), 2.19 (s, 3 H), 2.17 (s, 3 H), 1.38 (s, 9 H), 1.33 (br m, 2 H), 0.84 (s, 9 H); ^{13}C NMR (100 MHz, DMSO-d_6) δ 170.44, 169.62, 159.28, 139.21, 138.39, 137.04, 136.82, 135.14, 130.88, 81.28, 63.47, 56.65, 44.99, 44.79, 40.14, 33.25, 33.10, 31.96, 23.18, 18.84; HRMS-FAB (M + Na)$^+$ calcd for $C_{24}H_{40}N_7O_2Na$ 458.3243, found 458.3265.

2-Amino-4-(neohexylamino)-6-[(3-(aminomethyl)-4,6-dimethylbenzyl)amino]-1,3,5-triazine (8). Trifluoroacetic acid (3.5 mL) was added dropwise to a solution of the triazine derivative 7 (1 g, 2.12 mmol) in CH_2Cl_2 (15 mL) at 0 °C. The reaction mixture was warmed to 25 °C and stirred for 3 h. The solution was diluted with CH_2Cl_2 (150 mL), washed with 1 N NaOH (2 × 100 mL), dried over $MgSO_4$, filtered, and concentrated *in vacuo* to give 710 mg (1.98 mmol, 94%) of the product as a white crystalline solid: ^1H NMR (400 MHz, DMSO-d_6) δ 7.18 (s, 1 H), 6.87 (s, 1 H), 6.78, 6.59, 6.42, 6.23, 6.02, 5.87 (6 × br s, 4 H), 4.37 (br s, 1 H), 4.32 (br s, 1 H), 3.16 (br m, 4 H), 2.97 (br m, 2 H), 2.18 (br s, 6 H), 1.37 (br m, 2 H), 0.88 (br s, 9 H); ^{13}C NMR (100 MHz, DMSO-d_6) δ 170.15, 169.60, 141.91, 139.12, 136.83, 136.82, 135.05, 130.46, 46.80, 46.62, 44.71, 40.07, 33.07, 21.87, 21.64; HRMS-FAB (M + H)$^+$ calcd for $C_{19}H_{32}N_7$ 358.2719, found 358.2730.

Carbamic Acid, [3-[*N*-[2-[[4-Amino-6-[[[5-[[[4-amino-6[(3,3-dimethylbutyl)amino]-1,3,5-triazin-2-yl]amino]methyl]-2,4-dimethylphenyl]methyl]amino]-1,3,5-triazin-2-yl]amino]-5-bromobenzoyl]-*N*-[[4-(1,1-dimethylethyl)phenyl]methyl]amino]phenyl]-, 1,1-Dimethylethyl Ester (10). A solution of the amine 8 (1.05 g, 2.94 mmol), the triazine derivative 9 (2.0 g, 2.94 mmol), and DIPEA (2 mL) in DMA (35 mL) was heated at 85–90 °C for 4 h. The reaction mixture was concentrated *in vacuo*, and the residue was partitioned between EtOAc (100 mL) and brine (100 mL). The organic extract was washed with brine (2 × 50 mL), dried over $MgSO_4$, filtered, and concentrated *in vacuo*. The residue was purified by column chromatography (eluted with a solution of 5% NH_4OH/MeOH in $CHCl_3$ (1:9 v:v)) to give 1.72 g (1.72 mmol, 58%) of the product as a white crystalline foam: ^1H NMR (400 MHz, DMSO-d_6) δ 9.32 (br s, 1 H), 8.45 (br m, 2 H), 7.30 (br m, 5 H), 7.22–7.03 (br m, 5 H), 6.90 (s, 1 H), 6.62 (br s, 2 H), 6.50–5.90 (br m, 3 H), 4.99 (br s, 2 H), 4.36–4.31 (br m, 4 H), 3.16 (br m, 2 H), 2.22 (br s, 6 H), 1.39 (s, 9 H), 1.36 (br m, 2 H), 1.22 (s, 9 H), 0.86 (br s, 9 H); ^{13}C NMR (100 MHz, DMSO-d_6) δ 171.66, 170.70, 170.26, 169.58, 167.51, 156.08, 153.19, 146.25, 143.96, 142.12, 141.86, 139.10, 138.23, 137.66, 136.39, 136.08, 135.17, 134.76, 132.83, 130.97, 128.88, 126.72, 124.19, 120.00, 82.97, 56.26, 46.64, 41.12, 40.10, 38.16, 37.85, 34.78, 33.24, 33.05, 31.69, 25.01, 21.95; HRMS-FAB (M + H)$^+$ calcd for $C_{51}H_{66}BrN_{14}O_3$ 1001.4626, found 1001.4667.

2-[[4-Amino-6-[[[5-[[[4-amino-6-[(3,3-dimethylbutyl)amino]-1,3,5-triazin-2-yl]amino]methyl]-2,4-dimethylphenyl]methyl]amino]-1,3,5-triazin-

(31) Parris, C. L.; Christenson, R. M. *J. Org. Chem.* **1960**, *25*, 1888–1893.

2-yl]amino]-*N*-(3-aminophenyl)-*N*-[[4-(1,1-dimethylethyl)phenyl]methyl]-5-bromobenzamide (11). TFA (1 mL) was added dropwise to a solution of **10** (430 mg, 0.43 mmol) in CH_2Cl_2 (10 mL) at 0 °C. The reaction mixture was warmed to 25 °C and stirred for 2 h. The reaction mixture was diluted with PhMe (20 mL) and concentrated *in vacuo*. The residue was partitioned between EtOAc (50 mL) and 5% Na_2CO_3 solution (25 mL). The organic extract was washed with 5% Na_2CO_3 solution (25 mL) and brine (2 × 25 mL), dried over $MgSO_4$, filtered, and concentrated *in vacuo* to give 369 mg (0.41 mmol, 95%) of the product as a white crystalline foam: ^{1}H NMR (400 MHz, DMSO-d_6) δ 8.55 (br m, 2 H), 7.33–7.28 (m, 4 H), 7.22–7.16 (d, J = 2.1 Hz, 1 H), 6.91 (s, 1 H), 6.83 (br q, J = 7.9 Hz, 1 H), 6.64–6.42 (br m, 3 H), 6.31 (d, J = 8.1 Hz, 1 H), 6.24 (s, 1 H), 6.05–5.88 (br m, 1 H), 5.14 (br s, 2 H), 4.97 (s, 2 H), 4.34 (br m, 4 H), 3.16 (br m, 2 H), 2.23 (br s, 6 H), 1.35 (br m, 2 H), 1.23 (s, 9 H), 0.86 (br s, 9 H); ^{13}C NMR (100 MHz, DMSO-d_6) δ 171.62, 171.52, 170.71, 170.48, 169.57, 167.63, 167.48, 153.21, 153.09, 147.07, 146.97, 142.29, 142.09, 139.15, 138.81, 138.21, 137.93, 137.40, 135.99, 135.18, 134.65, 133.06, 132.58, 131.89, 130.85, 128.86, 117.64, 116.30, 115.35, 63.44, 56.33, 46.61, 44.78, 40.10, 37.86, 34.81, 33.06, 21.96, 18.06; HRMS-FAB $(M + H)^+$ calcd for $C_{46}H_{58}BrN_{14}O$ 901.4102, found 901.4086.

***N,N′,N″*-Tris[3-[*N*-[2-[[4-amino-6-[[[5-[[[4-amino-6-[(3,3-dimethylbutyl)amino]-1,3,5-triazin-2-yl]amino]methyl]-2,4-dimethylphenyl]methyl]amino]-1,3,5-triazin-2-yl]amino]-5-bromobenzoyl]-*N*-[[4-(1,1-dimethylethyl)phenyl]methyl]amino]phenyl]-1,3,5-benzenetricarboxamide (12) [Hub(MM)$_3$].** The amine **11** (350 mg, 0.39 mmol) was dissolved in CH_2Cl_2 (6 mL) and DIPEA (0.3 mL), and the solution was cooled to 0 °C. 1,3,5-Benzenetricarbonyl chloride (25 mg, 0.13 mmol) was added, and the solution was allowed to warm to 25 °C. After 45 min, the reaction mixture was diluted with CH_2Cl_2 (25 mL) and washed with 5% Na_2CO_3 (20 mL) and brine (2 × 35 mL), dried over $MgSO_4$, filtered, and concentrated *in vacuo*. The residue was purified by column chromatography (eluted with a solution of 5% NH_4OH/MeOH in CH_2Cl_2 (1:9 v:v)) to give 310 mg (0.108 mmol, 84%) of the product as a white solid: ^{1}H NMR (400 MHz, DMSO-d_6)[32] δ 10.60 (br s, 1 H), 8.62 (s, 1 H), 8.55 (br s, 1 H), 8.48-8.19 (2 × br s, 1 H), 7.75 (br s, 1 H), 7.60 (br m, 1 H), 7.30 (br m, 3 H), 7.20 (br m, 1 H), 7.14 (br s, 1 h), 6.86 (s, 1 H), 6.80–5.90 (br m, 6 H), 5.05 (br s, 2 H), 4.33 (br m, 4 H), 3.15 (br m, 2 H), 2.18 (br s, 6 H), 1.38 (br m, 2 H), 1.18 (s, 9 H), 0.82 (2 × br s, 9 H); ^{13}C NMR (100 MHz, DMSO-d_6)[33] δ 172.11, 170.68, 170.42, 169.56, 168.05, 167.21, 153.23, 143.34, 139.10, 138.81, 137.62, 137.34, 135.15, 130.89, 128.92, 127.38, 56.51, 46.59, 40.08, 37.84, 34.77, 33.17, 23.04, 21.93; LRMS-FAB $(M + H)^+$ calcd for $C_{147}H_{175}Br_3N_{42}O_6$ 2863, found 2863. Anal. Calcd for $C_{147}H_{172}Br_3N_{42}O_6$: C, 61.69; H, 6.02; Br, 8.38; N, 20.55. Found; C, 61.34; H, 5.89; Br, 8.07; N, 20.42.

Acknowledgment. This work was supported by The National Science Foundation (Grants CHE-91-22331 to G.M.W. and DMR-89-20490 to the Harvard University Materials Research Laboratory). NMR instrumentation was supported by the National Science Foundation Grant CHE-88-14019 and the National Institutes of Health Grant 1 S10 RR4870. Mass spectrometry was performed by Dr. A. Tyler. The Harvard University Mass Spectrometry Facility was Supported by The National Science Foundation Grant CHE-90-20043 and The National Institutes of Health Grant 1 S10 RR06716-01. We thank Professor Robert Cohen (MIT, chemical engineering) for the loan of his vapor pressure osmometer. J.P.M. was an SERC/NATO Postdoctoral Fellow, 1991–1993. C.T.S. was an Eli Lilly Predoctoral Fellow, 1991.

(32) Splitting of the *tert*-butyl resonances is the result of restricted rotations in the uncomplexed hub. These effects have been observed throughout out work with (neohexylamino)triazines and other (alkylamino)triazines.

(33) Only those resonances which were clearly identifiable are reported. The ^{13}C spectrum of hub(MM)$_3$ is complex due to the large number of different resonances in this rotationally restricted molecule.